MEDWIN PUBLISHERS
Committed to Create Value for researchers

Food Science & Nutrition Technology
ISSN: 2574-2701

Physical, Thermal and Spectroscopic Characterization of the Biofield Energy Treated Zinc Chloride

Trivedi MK[1] and Jana S[2]*

[1]Trivedi Global, Inc., Henderson, Nevada, USA

[2]Trivedi Science Research Laboratory Pvt. Ltd., Thane (W), India

***Corresponding author:** Snehasis Jana, Trivedi Science Research Laboratory Pvt. Ltd., Thane (W), Maharashtra, India, Tel: +91-022-25811234, Email: publication@trivedieffect.com

Research Article

Volume 5 Issue 3

Received Date: March 19, 2020

Published Date: May 12, 2020

DOI: 10.23880/fsnt-16000218

Abstract

Zinc is an important mineral for humans due to its role as an immune-booster, antioxidant and enzyme regulator. Zinc deficiency impairs growth and immunity. Zinc chloride is given as a dietary supplement in cases of zinc deficiency. The current study aimed to analyze the impact of the Trivedi Effect®- Energy of Consciousness Treatment on the physical, thermal, and spectral properties of zinc chloride. The methodology included dividing the zinc chloride sample into two equal parts; followed by keeping one part untreated and named as the Control sample. The other part was termed as the Biofield Energy Treated sample, which was remotely treated for ~3 minutes by Mr. Mahendra Kumar Trivedi, who was located in the USA, while the test samples were located in the research laboratory in India. Both the samples were analyzed using PXRD, PSA, DSC, UV-Vis, and FT-IR analytical techniques. The PXRD analysis revealed alterations in the relative peak intensities and crystallite sizes of the Treated sample in the range of 52.69% to 1232.65% and -33.36% to 92.28%, respectively, along with 13.75% significant increase in average crystallite size, compared with the Control sample. Also, the Biofield Energy Treated sample showed a significant increase in the particle sizes d_{10}, d_{50}, d_{90}, and D(4,3) values by 88.08%, 12.87%, 2.25%, and 9.13%, respectively, along with a 31.49% decrease in the surface area as compared to the Control sample. The DSC analysis revealed slight alterations in the melting and decomposition temperature of the Biofield Energy Treated sample by 0.59% and -1.22%, respectively; however, the latent heat of melting and decomposition significantly decreased by -7.41% and -68.41%, respectively, compared to the Control sample. Moreover, the FT-IR studies also revealed some alterations in the spectrum of the Biofield Energy Treated sample, as there were some additional peaks in the region of 650-1000 cm-1 and the Zn-Cl stretching peak was shifted to lower frequency i.e., 511 cm-1, compared to the Control sample (557 cm-1). The Energy of Consciousness Treatment may help in producing a new polymorphic form of zinc chloride, which may have better flowability, and storage parameters along with altered thermal stability compared to the untreated sample. Thus, the Biofield Energy Treated zinc chloride could be helpful in designing better nutraceutical, dietary supplements and/or pharmaceutical formulations to combat against zinc deficiency.

Keywords: Zinc Chloride; The Trivedi Effect®; Energy of Consciousness Treatment; PXRD; Particle Size; DSC; FT-IR

Introduction

Zinc is one of the 24 micronutrients needed for the survival of humans and it is considered as a vital mineral due to its requirement in the regulation of various enzymes. It acts as a cofactor for more than 300 enzymes that are responsible for the gene expression, signal transduction, and cell proliferation; and its deficiency may reduce the activity of such enzymes [1-3]. It also acts as an aphrodisiac, immune-booster and antioxidant supplement. The most common

reason for its use is to reduce the frequency of illness and to maintain the levels of testosterone in the body, to prevent issues that arise due to its deficiency [4].

Zinc mainly acts in the body as a prosthetic group for various metalloproteins enzymes. The superoxide dismustase enzyme is one among such enzymes which acts as an endogenous anti-oxidant and uses of both zinc and copper [5,6]. Moreover, zinc may also acts in the body by inhibiting the aromatase and reducing the level of estrogen, if given in very high doses. It also helps in maintaining the structure of proteins, nucleic acids, and cell membranes [7,8]. Its antioxidant properties are proved to be useful in solving prostate issues and it could be used in the repairing of intestinal mucosa. The other physiological functions involving the use of zinc are sexual maturation and reproduction [9], cell growth and division [10], wound-healing, adaptation in dark and night vision [11], and taste and olfactory sensitivity [12].

Oysters are a good source of zinc. Other food sources include eggs, meat, and legume products [13]. However, various studies reported that the nutrient content of these foods will be lost before their consumption, due to the use of chemical fertilizers and pesticides and cooking techniques. These factors create zinc deficiency which further causes hypogonadism, delayed growth, mental lethargy, diarrhea, hair loss, and skin abnormalities [14,15]. Research studies report that approximately 10% of the population of the USA are zinc deficient, as their dietary intake is less than 50% of the RDA [16]; whereas, global deficiency rates are more than 50%, because of high deficiency rates in the developing and undeveloped countries [17]. Moreover, the WHO has reported such deficiencies as a major factor associated with approximately 1.4% deaths in childhood, worldwide [18,19]. Therefore, zinc supplements such as, zinc chloride, are used for the prevention and treatment of zinc deficiency due to inadequate nutrition, intestinal malabsorption and other conditions that increase zinc loss from the body [20]. The Biofield Energy Treatment is considered as a novel approach which may help in improving the absorption and bioavailability of the compound.

Biofield Energy Treatments are an ancient practice, in which life force energy is transmitted by a Biofield practitioner. Biofield Energy is a dynamic low-level electromagnetic field surrounding the human body [21,22]. Biofield Energy is infinite, para-dimensional and can freely flow between the human and the environment. The National Center of Complementary and Integrative Health (NCCIH) has recognized and accepted Biofield Energy Treatments as a CAM approach in addition to other therapies, medicines and practices [23-25]. Thus, a human has the ability to harness energy from the universe and can transmit it to any living organism(s) or non-living object(s) around the globe. The object or recipient receives the energy and responds in a useful way. This process is known as the Trivedi Effect® - Biofield Energy Treatment [26,27]. The Trivedi Effect® has been reported transforming the physiochemical properties of various pharmaceuticals [28-30], alter the isotopic composition of the organic compounds [31-33], nutraceuticals [34-36], alter the properties of metals and ceramics in materials science [37,38], improve agricultural crop productivity [39,40], and modulate the efficacy in different living cells [41,42]. Thus, this study was designed to investigate the impact of the Biofield Energy Treatment (the Trivedi Effect®) on the physicochemical, thermal and spectroscopic properties of zinc chloride with the help of various analytical techniques such as, powder X-ray diffraction (PXRD), particle size analysis (PSA), differential scanning calorimetry (DSC), thermogravimetric analysis (TGA), UV-visible, and FT-IR spectroscopy.

Materials and Methods

Chemicals and Reagents

Zinc chloride was procured from Tokyo Chemical Industry Co., Ltd. (TCI), Japan. All other chemicals used in the experiment were of analytical grade available in India.

Consciousness Energy Healing Treatment Strategies

In this treatment strategy, the zinc chloride test compound was divided into two parts. One part did not receive the Biofield Energy Treatment and was termed the Control sample. The other part of zinc chloride was considered as Treated sample, which received the Energy of Consciousness Treatment remotely for ~3 minutes through the unique Energy Transmission process Mr. Mahendra Kumar Trivedi, who was located in the USA, while the test samples were located in the research laboratory in India. The Control zinc chloride was subjected to a "sham" healer (who did not have any knowledge about the Biofield Energy Treatment) under similar laboratory conditions. The Control and the Biofield Energy Treated zinc chloride samples were kept in similar sealed conditions and further characterized by using PXRD, PSA, DSC, UV-Vis, and FT-IR techniques.

Characterization

Powder X-ray Diffraction (PXRD) Analysis

The PXRD analysis of the Control and the Biofield Energy Treated samples of zinc chloride was completed with a PA Nalytical X'Pert3 powder X-ray diffractometer (UK). A copper line was used as the radiation source for diffracting the analyte at 0.154 nm X-ray wavelengths, which is running at 40 mA current and 45 kV voltages. The scanning rate for

the instrument was kept at 18.87°/second over a 2θ range of 3-90° and the ratio of Kα-2 and Kα-1 was 0.5 (k, equipment constant). The data produced by the instrument was collected an X'Pert data collector and X'Pert high score plus processing software. It provides the data in the form of a chart of the Bragg angle (2θ) *vs.* intensity (counts per second), and a table providing information regarding the peak intensity counts, d value (Å), full width half maximum (FWHM) (°2θ), relative intensity (%), and area (cts*°2θ). From this data, the crystallite size (G) was analyzed with the Scherrer equation (1) as follows:

$$G = k\lambda / (bCos\theta) \quad (1)$$

Where k is the equipment constant (0.5), λ is the X-ray wavelength (0.154 nm); b in radians is the full-width at half of the peaks and θ is the corresponding Bragg angle.

The percentage change in the crystallite size (G) of zinc chloride was calculated using following equation 2:

$$\%\,Change\,\text{s in}\,crystallite\ size = \frac{\left[G_{Treated} - G_{The\ Control}\right]}{G_{The\ Control}} \times 100 \quad (2)$$

Where, $G_{Control}$ and $G_{Treated}$ are the crystallite sizes of the Control and the Biofield Energy Treated zinc chloride samples, respectively.

Particle Size Analysis (PSA)

The particle size analysis was done using the wet method, which involves the use of a Malvern Mastersizer 3000 (UK) instrument. The instrument has a detection range between 0.01 µm to 3000 µm [43], and the method involves the filling of sample unit (Hydro MV) with light liquid paraffin oil, which acts as dispersant medium. The refractive index values for the dispersant medium and samples were 0.0 and 1.47, respectively. It was stirred at 2500 rpm, and the measurement was taken twice after reaching obscuration in between 10% and 20%, followed by averaging both measurements. The PS analysis provided data in the form of d_{10}µm, d_{50}µm, and d_{90}µm values, representing the particle diameter corresponding to 10%, 50% and 90% of the cumulative distribution. D (4,3) µm value represents the average mass-volume diameter and SSA is the specific surface area (m^2/Kg). The calculations were done by Mastersizer V3.50 software.

The percentage change in particle size (d) for d_{10}, d_{50}, d_{90} and D (4,3) was calculated using following equation 3:

$$\%\,Change\,\text{in}\,particle\ size = \frac{\left[d_{Treated} - d_{Control}\right]}{d_{Control}} \times 100 \quad (3)$$

Where, $d_{Control}$ and $d_{Treated}$ are the particle size (µm) for at below 10% level (d_{10}), 50% level (d_{50}), and 90% level (d_{90}) of the Control and the Biofield Energy Treated samples, respectively.

Percentage change in surface area (S) was calculated using following equation 4:

$$\%\,Change\,\text{in}\,surface\ area = \frac{\left[S_{Treated} - S_{Control}\right]}{S_{Control}} \times 100 \quad (4)$$

Where, $S_{Control}$ and $S_{Treated}$ are the surface area of the Control and the Biofield Energy Treated zinc chloride samples, respectively.

Differential Scanning Calorimetry (DSC)

The DSC analysis of the samples was done under a dynamic nitrogen atmosphere using a DSC Q2000 differential scanning calorimeter (USA) at the flow rate of 50 mL/min. In this process, a 2-4 mg sample was weighed and sealed in aluminium pans. The sample was equilibrated at 30°C followed by heating up to 450°C at the rate of 10°C/min under nitrogen gas as purge atmosphere [44]. The thermogram revealed the value for onset, end set, peak temperature, peak height (mJ or mW), peak area, and change in heat (J/g) for each peak. The percentage change in melting temperature (T) of the Control and the Biofield Energy Treated samples was calculated using following equation 5:

$$\%\,Change\,\text{in}\,melting\ \ temperature = \frac{\left[T_{Treated} - T_{Control}\right]}{T_{Control}} \times 100 \quad (5)$$

Where, $T_{Control}$ and $T_{Treated}$ are the melting temperature of the Control and the Biofield Energy Treated zinc chloride samples, respectively.

Also, the percentage change in the latent heat of fusion (ΔH) was calculated using following equation 6:

$$\%\,Change\,\text{in}\,latent\ \ heat\ \ of\ \ fusion = \frac{\left[\Delta H_{Treated} - \Delta H_{Control}\right]}{\Delta H_{Control}} \times 100 \quad (6)$$

Where, $\Delta H_{Control}$ and $\Delta H_{Treated}$ are the latent heat of fusion of the Control and the Biofield Energy Treated zinc chloride samples, respectively.

Ultraviolet-Visible Spectroscopy (UV-Vis) Analysis

The UV-Vis spectral analysis of the Control and the Biofield Energy Treated zinc chloride samples was done using a Shimadzu UV-2400PC SERIES with UV Probe (Shimadzu, JAPAN). The spectrum was recorded in the wavelength range

of 190-800 nm using 1 cm quartz cell having a slit width of 0.5 nm. The absorbance spectra (in the range of 0.2 to 0.9) and wavelength of maximum absorbance (λ_{max}) were recorded.

Fourier Transform Infrared (FT-IR) Spectroscopy

FT-IR spectroscopy of zinc chloride was done using a Spectrum ES Fourier transform infrared spectrometer (Perkin Elmer, USA) with the frequency array of 400-4000 cm^{-1}. The process involves pressed KBr disk technique in which, ~2 mg of sample was taken along with about 300 mg of KBr as the diluent, followed by forming the pressed disk and running the sample in the spectrometer.

Results and Discussion

Powder X-ray Diffraction (PXRD) Analysis

The PXRD diffractograms of the Control and the Biofield Energy Treated samples of zinc chloride are shown in Figure 1. The diffractograms of both the samples showed sharp peaks representing the crystalline nature of both the samples. The data regarding PXRD analysis is presented in Table 1 that includes the details regarding Bragg angle (2θ), relative peak intensity (%), and crystallite size (G) for the Control and the Biofield Energy Treated zinc chloride samples. Moreover, the crystallite size was calculated using Scherrer equation [45].

The analysis revealed that the crystallite sizes of the Biofield Energy Treated sample at 2θ equal to nearly 15.7°, 16.6°, 38.3°, 48.8° and 61.8° (Table 1, entry 1, 2, 6, 7, and 12) showed a slight reduction as compared to the Control sample. However, the crystallite sizes of the Biofield Energy Treated zinc chloride at 2θ equal to nearly 52.3° and 56.3° (Table 1) (entry 9 and 10) were significantly decreased by 33.36% and 20.02%, respectively, compared with the Control sample. Consequently, the crystallite sizes at the 2θ positions 25.6°, 29.4°, 35.1°, 49.3°, and 58.4° (Table 2) (entry 3-5, 8, and 11) of the Biofield Energy Treated sample were significantly increased in the range from 24.96% to 92.28% as compared to the Control sample. The average crystallite sizes of the Control and the Biofield Energy Treated zinc chloride were 63.77 and 72.54 nm, respectively. Thus, the average crystallite size was significantly increased by 13.75% in the Biofield Energy Treated sample in comparison to the Control sample. The reason behind this alteration might be attributed to the Biofield Energy which might induce the movement of crystallite boundaries that further causes the crystal growth and thereby increased crystallite size [46].

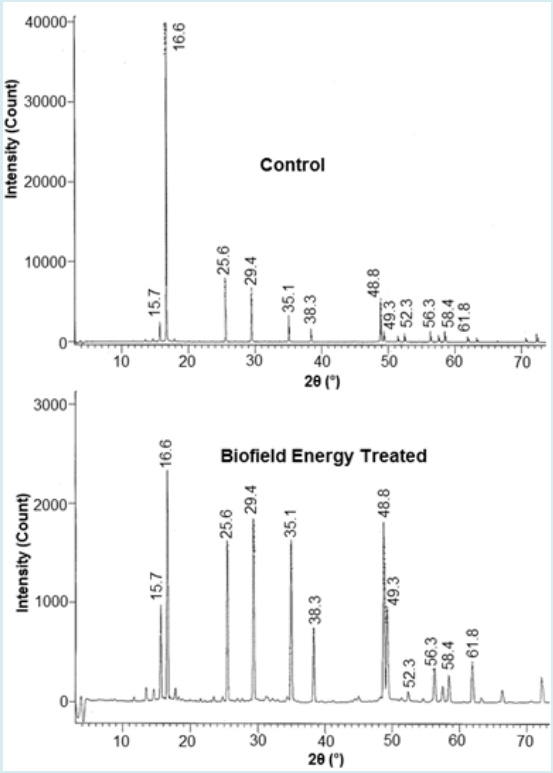

Figure 1: PXRD diffractograms of the Control and the Biofield Energy Treated zinc chloride.

Entry No.	Bragg angle (°2θ)	Relative Peak Intensity (%)			Crystallite size (G, nm)		
		Control	Treated	% change [a]	Control	Treated	% change [b]
1	15.7	6.19	41.82	575.61	43.43	43.43	-0.01
2	16.6	100	100	0.00	49.71	49.70	-0.01
3	25.6	10.23	60.7	493.35	50.16	96.45	92.28
4	29.4	7.91	78.74	895.45	50.58	72.93	44.19
5	35.1	4.38	58.37	1232.65	51.31	98.66	92.27
6	38.3	4.23	31.03	633.57	74.71	74.69	-0.02
7	48.8	12.78	76.19	496.17	77.49	77.47	-0.02
8	49.3	3.35	39.16	1068.96	62.12	77.63	24.96

9	52.3	2.79	4.26	52.69	78.65	52.42	-33.36
10	56.3	3.36	14.88	342.86	80.05	64.02	-20.02
11	58.4	3.25	11.03	239.38	64.70	80.85	24.96
12	61.8	1.76	16.29	825.57	82.31	82.28	-0.03

Table 1: PXRD data for the Control and the Biofield Energy Treated zinc chloride.

a) Denotes the percentage change in the relative intensity of the Biofield Energy Treated sample with respect to the Control sample;

b) Denotes the percentage change in the crystallite size of the Biofield Energy Treated sample with respect to the Control sample.

Test Item	d_{10} (µm)	d_{50} (µm)	d_{90} (µm)	D(4,3) (µm)	SSA (m^2/Kg)
Control sample	4.70	94.80	178.0	95.30	350.30
Biofield Energy Treated sample	8.84	107.0	182.0	104.0	240.0
Percent change* (%)	88.08	12.87	2.25	9.13	-31.49

Table 2: Particle size distribution of the Control and the Biofield Energy Treated zinc chloride.

Besides, the PXRD diffractogram of both the samples, *i.e.,* the Control and the Biofield Energy Treated zinc chloride showed the highest peak intensity (100%) at Bragg's angle (2θ) equal to 16.6° (Table 1, entry 2). The other peaks of the Biofield Energy Treated sample's diffractogram showed a significant increase in their relative peak intensities in the range from 52.69% to 1232.65%, compared to the Control sample. The literature reported that the relative intensity across each plane of the crystalline compound may vary based on the crystal morphology [47]. Also, the increased relative intensity of the characteristic peaks suggested that the crystallinity of the Biofield Energy Treated sample might be increased as compared to the Control sample. Thus, it is presumed that the Biofield Energy might induce the formation of a more symmetrical crystalline long range pattern after getting absorbed by the Biofield Energy Treated sample that caused the increase in intensity of peaks. Hence, the energy transferred *via* the Biofield Energy Healing Treatment probably altered the size and shape of molecules, thereby altering the crystallinity and crystallite size of the Treated sample as compared to the Control sample. Moreover, some studies mentioned the changes in XRD pattern as the sign of polymorphic transitions [48,49] which may further affects the solubility, dissolution, and bioavailability parameters of the drug [50]. Hence, the PXRD study revealed that the Biofield Energy Treatment might produce a new polymorphic form of zinc chloride, which could have altered bioavailability profile as compared with the Control sample.

Particle Size Analysis (PSA)

The particle size and surface area of the Control and the Biofield Energy Treated zinc chloride were analyzed and are presented in Table 2. The particle size distribution of the Control sample was observed at d_{10} (4.70µm), d_{50} (94.80µm), d_{90} (178.0µm), and D (4,3) (95.30µm). The particle size distribution of the Biofield Energy Treated sample at d_{10}, d_{50}, d_{90}, and D (4,3) was found as 8.84µm, 107.0µm, 182.0µm, and 104.0µm, respectively. The analysis revealed that the particle size values at d_{10}, d_{50}, d_{90}, and D (4,3) in the Biofield Energy Treated zinc chloride were significantly increased by 88.08%, 12.87%, 2.25%, and 9.13%, respectively as compared with the Control sample. However, the specific surface area (SSA) of the Biofield Energy Treated zinc chloride (240.0m^2/Kg) was significantly decreased by 31.49% with respect to the Control sample (350.30m^2/Kg). The reason behind this decrease in surface area might be attributed to the increased particle size of the Treated sample after the Biofield Energy Treatment [51]. According to some previous studies, the particle size of compound may increase along with increase in the thermal energy. Thus, it is presumed that the Biofield Energy Treatment might act in this way and reduced the thermodynamically driving force, which caused the decrease in nucleus densities and thereby enhanced the particle size [52,53]. This increased particle size of the Biofield Energy Treated sample might be useful in enhancing the appearance, shape and flowability of the compound [54,55].

d_{10}, d_{50}, and d_{90}: particle diameter corresponding to 10%, 50%, and 90% of the cumulative distribution, D (4,3) : the average mass-volume diameter, SSA : the specific surface area; *denotes the percentage change in the particle size distribution of the Biofield Energy Treated sample with respect to the Control sample.

Differential Scanning Calorimetry (DSC) Analysis

The DSC thermograms of the Control and the Biofield Energy Treated zinc chloride are presented in Figure 2.

The melting/decomposition temperature and enthalpy of fusion/decomposition of the Control and the Biofield Energy Treated zinc chloride are also presented in the Table 3. The melting/fusion temperature was slightly increased by 0.59% in the Treated zinc chloride (312.57°C) as compared to the Control sample (309.52°C). The onset and end set melting temperatures of the Treated sample also showed slight alterations by 0.99% and -0.61%, respectively compared with the Control sample.

Peak	Description	T_{onset} (°C)	T_{peak} (°C)	T_{endset} (°C)	ΔH (J/g)
Endothermic peak	Control sample	309.52	313.42	321.92	9.612
	Biofield Treated sample	312.57	315.26	319.95	8.90
	% Change	0.99	0.59	-0.61	-7.41
Exothermic peak	Control sample	388.23	390.27	395.08	189.90
	Biofield Treated sample	383.81	385.50	396.07	59.98
	% Change	-1.14	-1.22	0.25	-68.41

Table 3: The latent heat of fusion (J/G) and melting point (°C) values of the Control and the Biofield Energy Treated zinc chloride.

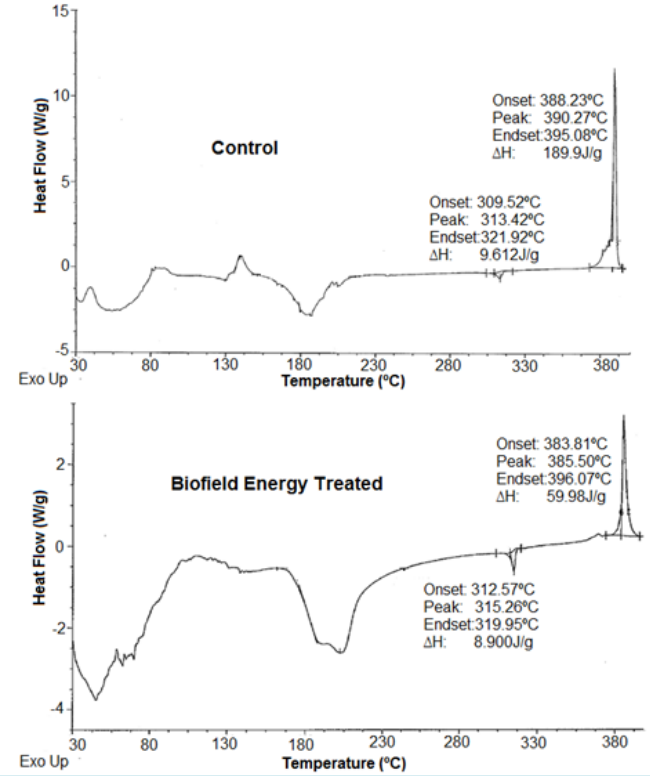

Figure 2: DSC thermograms of the Control and the Biofield Energy Treated zinc chloride.

The enthalpies of fusion (ΔHfusion) of the Control and Treated zinc chloride were 9.612 J/g and 8.90 J/g, respectively. The ΔH_{fusion} of the Treated sample was decreased significantly by 7.41% compared with the Control sample. The decomposition temperature of the Treated zinc chloride (385.50°C) was decreased by 1.22%, compared to the Control sample (390.27°C). The onset and end set decomposition temperatures of the Biofield Energy Treated sample also showed slight alterations by -1.14% and 0.25%, respectively compared with the Control sample. The enthalpies of decomposition (ΔHdecomposition) of the Control and Treated zinc chloride were 189.90J/g and 59.98 J/g, respectively. The $\Delta H_{decomposition}$ of the Treated sample was significantly decreased by 68.41% compared with the Control sample.

In a solid, the atomic bonds possess a considerable quantity of the interaction forces that help in holding the atoms at their positions. Hence, there is the need of a sufficient amount of energy to change the solid phase compound in the form of liquid, which is known as the latent heat of fusion (ΔH). Also, the energy supplied to the compound during this phase change *i.e.* ΔH is stored by the atoms in the form of potential energy [56]. In the Biofield Energy Treated sample, the reduction in ΔH revealed that Treated sample might possess some extra internal energy in the form of potential energy as compared to the Control that might be transferred in the sample through the Biofield Energy Treatment. Thus, it is presumed that the Biofield Energy Treatment might increase the internal energy in the Treated zinc chloride that leads to reduced enthalpy of fusion/decomposition and altered thermal stability of the Biofield Energy Treated sample. This alteration in the thermal stability might be advantageous in long term storage and shipping of the compound [57].

Ultraviolet-Visible Spectroscopy (UV-Vis) Analysis

The UV-visible spectra of both, the Control and the Biofield Energy Treated zinc chloride samples are presented in Figure 3.

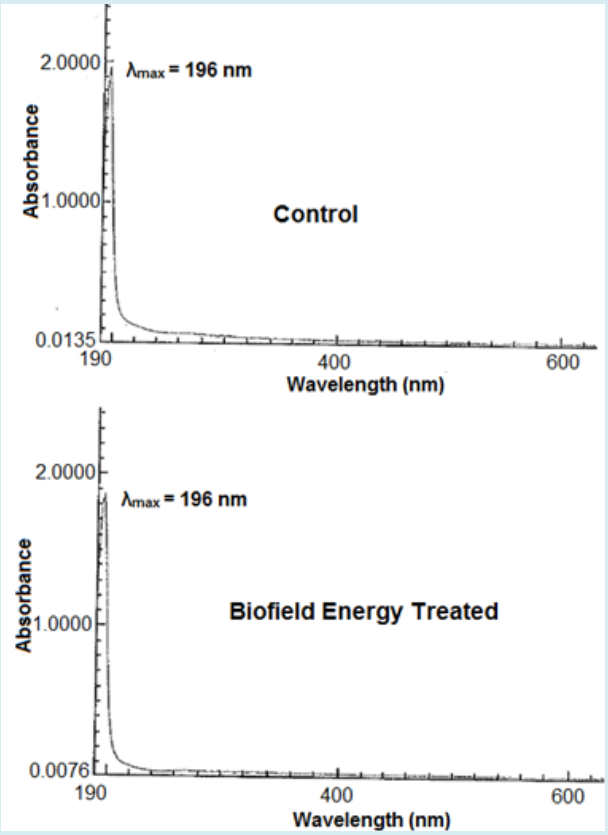

Figure 3: UV-vis spectra of the Control and the Biofield Energy Treated zinc chloride.

The UV-Vis spectra showed the wavelength of the most intense UV-Vis absorbance (λ_{max}) at 196.0 nm in both the Control and the Biofield Energy Treated samples (Figure 3) with a minor shift of absorbance maxima from 1.9590 (the Control) to 1.8707 in the Treated sample. The spectra arise due to the UV absorbance occurring through various energy transitions from the ground to the excited state such as $\sigma \rightarrow \sigma^*$, $n \rightarrow \pi^*$, and $\pi \rightarrow \pi^*$ [58]. The UV-vis spectroscopic analysis of zinc chloride revealed the similar spectra with no significant alteration in the λ_{max} between the Control and the Biofield Energy Treated sample.

The UV-Vis spectroscopy provides the basic information regarding the skeleton of chemical structure as well as the arrangement of functional groups on the chemical structure [59]. Thus, the analysis revealed that the structural configuration of both the samples was remained same.

Fourier Transform Infrared (FT-IR) Spectroscopy

The FT-IR spectra of the Control and the Biofield Energy Treated samples of zinc chloride are presented in the Figure 4.

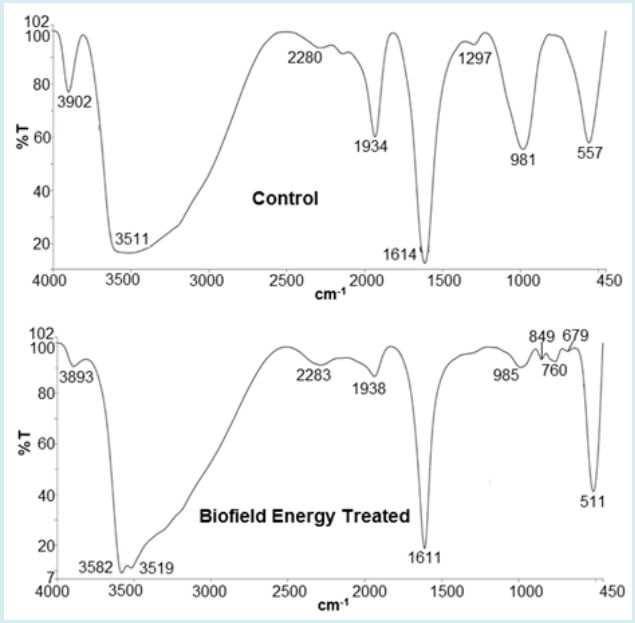

Figure 4: FT-IR spectra of the Control and the Biofield Energy Treated zinc chloride.

The characteristic peaks were observed at 3511, 1934, 1614, 981, and 557 cm^{-1} in the Control FT-IR spectrum (Figure 4). The FT-IR spectrum of the Biofield Energy Treated zinc chloride (Figure 4) showed the characteristic peaks at 3582, 3519, 1938, 1611, 985, 760, and 511 cm^{-1}. The spectrum of the Control sample showed strong and broad absorption band at 3511 cm^{-1} and at 1614 cm^{-1} (H-O-H bending) that might be due to the presence of the lattice water (Figure 4). In the spectrum of the Biofield Energy Treated zinc chloride, the peaks for the lattice water were observed at 3582, 3519, and 1611 cm^{-1}. The literature reported that the metal stretching absorption band in case of inorganic materials was found in the frequency region 750-1000 cm^{-1} [60]. In the spectrum of the Control sample, this metal-halogen (Zn-Cl) stretching peak was observed at 557 cm^{-1}, whereas it was shifted downward in the Biofield Energy Treated sample at 511 cm^{-1}. Also, there were some additional peaks in the region of 650-1000 cm^{-1}. According to the literature, the peak frequency (ν) for any bond is directly proportional to its bond force constant (k), which is further inversely related to the average bond length (r) [61]. Hence, it is anticipated that the shifting of peak wave number corresponding to the aromatic Zn-Cl bond could be due to alteration in the corresponding bond length after the Biofield Energy Treatment. Overall, the FT-IR results suggest that the Biofield Energy Treatment might affect the atomic level of zinc chloride, which may cause some alterations in the structural and bonding properties such as, bond strength, rigidity of structure, and the stability of compound, etc.

Conclusion

Overall, the study showed the effect of the Trivedi Effect® - Energy of Consciousness Treatment on the physical, thermal and spectroscopic properties of zinc chloride. The PXRD data showed alterations in the crystallite sizes and relative intensities across various planes of the Biofield Energy Treated zinc chloride sample as compared to the Control sample. The Biofield Energy Treated sample showed an increase in the relative intensities in the range from 52.69% to 1232.65%, in comparison to the Control sample. Also, the crystallite sizes of the Biofield Energy Treated sample showed significant alterations in the range from -33.36% to 92.28% with 13.75% a significant increase in the average crystallite size, when compared with the Control sample. Such alterations suggest changes in the crystallinity and crystal morphology of the Biofield Energy Treated sample along with the polymorphic form of the zinc chloride sample. Additionally, the particle size values of the Biofield Energy Treated zinc chloride sample at d_{10}, d_{50}, d_{90}, and D(4,3) were significantly increased by 88.08%, 12.87%, 2.25%, and 9.13%, respectively as compared with the Control sample. This alteration in particle size also affected the specific surface area of the Biofield Energy Treated sample, which was significantly reduced by 31.49%, in comparison to the Control sample. The increased particle size of the Biofield Energy Treated zinc chloride may help in increasing the appearance, shape, flowability, and stability profile. The melting and decomposition temperatures of the Biofield Energy Treated sample were slightly altered by 0.59% and -1.22%, respectively, whereas, the ΔH_{fusion} and $\Delta H_{decomposition}$ were significantly reduced by -7.41% and -68.41%, respectively, compared to the Control sample. It revealed that the thermal stability of the Treated zinc chloride sample was altered, compared with the Control sample. The FT-IR spectrum of the Biofield Energy Treated sample showed alterations in the frequencies of peaks, as the peak corresponding to Zn-Cl stretching was shifted to lower frequency *i.e.,* 511 cm^{-1}, compared to the Control sample (557 cm^{-1}). Also, there were some additional peaks in the region of 650-1000 cm^{-1}, when compared with the spectrum of the Control sample. Thus, the study concluded that the Energy of Consciousness Treatment may change the crystallinity and polymorphic form of zinc chloride, which could provide a better appearance, flowability, and storage profile with altered thermal stability. Hence, the Energy of Consciousness Treatment could be very useful in designing better nutraceutical and dietary supplement formulations for the treatment of various deficiencies and disorders, such as, arrhythmias, gestational hypertension, cancer, inflammatory diseases, septic shock, diabetes mellitus, allergies, immunological disorders, asthma, etc.

Acknowledgement

The authors are grateful to GVK Biosciences Pvt. Ltd., Trivedi Science, Trivedi Global, Inc., and Trivedi Master Wellness for their assistance and support during this work.

References

1. Prasad AS (1995) Zinc: An overview. Nutrition 11: 93-99.
2. Vallee BL, Falchuk KH (1993) The biochemical basis of zinc physiology. Physiol Rev 73(1): 79-118.
3. Haase H, Rink L (2009) Functional significance of zinc-related signaling pathways in immune cells. Annu Rev Nutr 29: 133-152.
4. Prasad AS (2008) Clinical, immunological, anti-inflammatory and antioxidant roles of zinc. Exp Gerontol 43(5): 370-377.
5. Anzellotti AI, Farrell NP (2008) Zinc metalloproteins as medicinal targets. Chem Soc Rev 37(8): 1629-1651.
6. Abreu IA, Cabelli DE (2010) Superoxide dismutases-a review of the metal-associated mechanistic variations. Biochim Biophys Acta 1804(20: 263-274.
7. McClain C (1981) Trace metal abnormalities in adults during hyperalimentation. JPEN 5(5): 4244-4249.
8. Kappas A, Sassa S, Anderson K (1983) The porphyrias. In: The metabolic basis of inherited disease, 5th (Edn.), Stanbury J, Wyngaarden J, Frederickson D, Brown M, McGraw-Hill, (Eds.), New York.
9. Prasad A (1991) Discovery of human zinc deficiency and studies in an experimental human model. Am J Clin Nutr 53: 403-412.
10. Solomons N (1984) Zinc. In: Clinical guide to parenteral micronutrition, 1st (Edn.), Educational Publications, Baumgartner TG.
11. Sandstead H (1985) Zinc: Essentiality for brain development and function. Nutr Rev 43(5): 129-137.
12. Russell RM, Cox ME, Solomons N (1983) Zinc and the special senses. Ann Int Med 99(2): 227-239.
13. Gueguen M, Amiard JC, Arnich N, Badot PM, Claisse D, et al. (2011) Shellfish and residual chemical contaminants: Hazards, monitoring, and health risk assessment along French coasts. Rev Environ Contam Toxicol 213: 55-111.

14. Behrens R, Tomkins A, Roy S (1990) Zinc supplementation during diarrhea, a fortification against malnutrition? Lancet 336(8712): 442-443.

15. Prasad AS (1985) Clinical manifestations of zinc deficiency. Annu Rev Nutr 5: 341-363.

16. Cope EC, Levenson CW (2010) Role of zinc in the development and treatment of mood disorders. Curr Opin Clin Nutr Metab Care 13(6): 685-689.

17. Takeda A, Tamano H (2009) Insight into zinc signaling from dietary zinc deficiency. Brain Res Rev 62(1): 33-44.

18. The world health report (2002) Quantifying selected major risks to health. reducing risks, promoting healthy life.

19. Hambidge M (2000) Human zinc deficiency. J Nutr 130 (S5): S1344-S1349.

20. Maret W, Sandstead HH (2006) Zinc requirements and the risks and benefits of zinc supplementation. J Trace Elem Med Biol 20(1): 3-18.

21. Rubik B, Muehsam D, Hammerschlag R, Jain S (2015) Biofield Science and Healing: History, Terminology, and Concepts. Global Advances in Health and Medicine 4: 8-14.

22. Warber SL, Cornelio D, Straughn, J, Kile G (2004) Biofield energy healing from the inside. J Altern Complement Med 10: 1107-1113.